Synthesis of Stable Hybrid Silica-Lipid Cylinders with Nanoscale Helical Ripples

DATASET · JANUARY 2011

CITATIONS
2

READS
8

4 AUTHORS, INCLUDING:

Yue Zhao
University of Iowa
18 PUBLICATIONS **376** CITATIONS
SEE PROFILE

Yongho Sohn
University of Central Florida
169 PUBLICATIONS **2,073** CITATIONS
SEE PROFILE

Synthesis of Stable Hybrid Silica−Lipid Cylinders with Nanoscale Helical Ripples

Yue Zhao, Jing Liu, Yongho Sohn, and Jiyu Fang*

Advanced Materials Processing and Analysis Center and Department of Mechanical, Materials, and Aerospace Engineering, University of Central Florida, Orlando, Florida 32816

Received: December 12, 2006; In Final Form: February 20, 2007

Self-assembled cylindrical lipid tubules have attracted attention as templates for synthesizing hybrid organic−inorganic materials. Here we report the synthesis of hybrid silica−lipid cylinders by sol−gel condensation of tetraethoxysilane (TEOS) on helical rippled tubules of 1,2-bis(tricosa-10,12-diynoyl)-*sn*-glycero-3-phosphocholine ($DC_{8,9}PC$). Transmission electron microscopy reveals that the nanoscale helical ripples of the lipid tubules are transcripted to the templated silica films. On the other hand, the deposition of the silica films substantially improves the thermal stability of lipid tubules. We find that the crystalline ordering of lipid bilayer walls confined in the hybrid silica−lipid cylinders is stable up to 110 °C.

1. Introduction

Molecular self-assembly is becoming increasingly popular as a "bottom-up" approach to synthesize technologically useful nanostructures.[1] One of the most attractive aspects of this approach is the prospect of assembling structures with molecular precision under experimentally straightforward and inexpensive conditions. Recently, there has been a great interest in using the self-assembled supramolecular structures of amphiphilic surfactants as templates for synthesizing ordered silica structures because of their potential applications in catalysis, separation technology, photonics, and bioengineering.[2,3] Self-assembled lipid tubules are hollow cylinders, composed of rolled-up lipid bilayer sheets.[4,5] The hollow cylindrical shape and crystalline molecular order of bilayer walls make lipid tubules attractive as templates for the synthesis of functional materials with controlled shapes and sizes.[6−12] Baral and Schoen[13] reported the formation of silica hollow cylinders by the gel of ∼10 nm silica colloidal particles on lipid tubules of 1,2-bis(tricosa-10,-12-diynoyl)-*sn*-glycero-3-phosphocholine ($DC_{8,9}PC$). However, the templated silica hollow cylinders have thick walls. Shimizu and co-workers[14,15] found that silica hollow cylinders with ultrathin walls could be formed by direct sol−gel reaction of tetraethoxysilane (TEOS) on the nanotubes of amino acid based and cholesterol-based lipids. Mann and co-workers[16] synthesized silica−lipid lamellar tubules by carrying out the acid hydrolysis and condensation of TEOS coupled with the self-assembly of $DC_{8,9}PC$ in solution.

The ripple phase, which is characterized by corrugations with defined periodicities, is one of the most intriguing phases in lipid bilayer membranes.[17] Selinger et al. developed a theoretical mode based on chiral interactions coupled with molecular tilt for describing the formation of chiral lipid tubules.[18] They predicted that the modulated tilt order of chiral lipids could induce helical ripples in tubular walls. Recently, we imaged the molecular tilt ordering in $DC_{8,9}PC$ tubules with liquid-crystal optical amplification and confirmed the predicted modulated tilt state in which the molecular tilt director gradually changes to form helical stripes separated by sharp defect lines.[19] By using atomic force microscopy (AFM), we observed the modulated-tilt-induced helical ripples in the cylindrical bilayer walls of $DC_{8,9}PC$ tubules.[20] The helical ripples were also reported in lipid tubules of 1,2-dimyristoyl-*sn*-glycero-3-phosphatidylcholine (DMPC) by Lauf et al.[21] They found that the ripples had a period of 23 nm and run along the equator of the DMPC tubules. Here we report the synthesis of hybrid silica−lipid cylinders by the sol−gel reaction of TEOS on rippled $DC_{8,9}PC$ tubules in acid solution. Transmission electron microscopy (TEM) reveals that the nanoscale helical ripples of $DC_{8,9}PC$ lipid tubules are transcripted to the templated silica cylinders. Although the transcription of lipid tubules into silica cylinders has been reported in the literature,[13−16] this is the first discovery to our knowledge of transcripting the nanoscale helical ripples into the templated silica cylinders. The surface area of the rippled silica cylinders is large compared with that of the smooth silica cylinders with the same diameter. The templated silica cylinders with nanoscale helical ripples are expected to have potential applications in heterogeneous chiral catalysis and separation. In addition, the deposition of the silica film substantially improves the thermal stability of lipid tubules. We find that the crystalline ordering of lipid bilayer walls in the hybrid silica−lipid cylinders is stable up to 110 °C.

2. Experimental Section

Lipid tubules were prepared by thermal cycling of 5 mg/mL suspension of 1,2-bis(tricosa-10,12-diynoyl)-*sn*-glycero-3-phosphocholine ($DC_{8,9}PC$) (Avanti Polar Lipids, Alabaster, AL) in ethanol/water (70:30 v/v) from 60 °C to room temperature at a rate of ∼0.5 °C/min. The polymerization of $DC_{8,9}PC$ tubules was performed with UV irradiation (254 nm) for 20 min at room temperature. Tetraethoxysilane (TEOS) was obtained from Aldrich and used as received. In our experiments, 20.6 μL of TEOS was first added to 2 mL of $DC_{8,9}PC$ tubule suspension. A solution (1.8 mL), which was prepared from H_2O (50 mL) and 35.5 wt % aqueous HCl (10 μL), was added to the tubule/TEOS mixture. The mixture was allowed to stand undisturbed at room temperature for 1 week and then centrifuged at 5000 rpm for 10 min, and the supernatant was decanted. A drop of solution containing the hybrid silica−lipid cylinders was placed on carbon-coated grids and Au-coated mica substrates and then dried in air at room temperature. Atomic force

* Corresponding author. Email: jfang@mail.ucf.edu.

10.1021/jp0685479 CCC: $37.00
Published on Web 04/12/2007

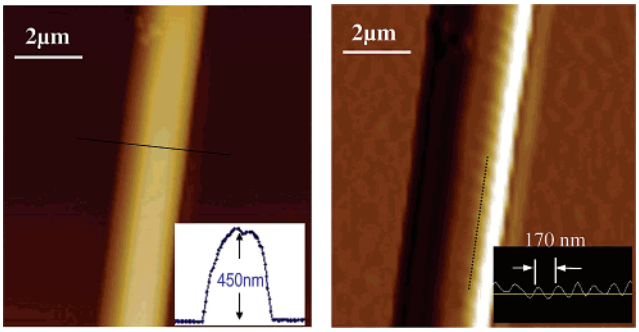

Figure 1. (a, left) Height and (b, right) amplitude mode images of a $DC_{8,9}PC$ tubule on a glass substrate. These images were taken simultaneously. The high profile along the dark line is inset in (a). The amplitude profile along the dark line is inset in (b).

microscopic images of $DC_{8,9}PC$ tubules adsorbed on substrates were taken with a DI Dimension 3100 microscope (Digital Instruments) in air at room temperature. Silicon nitride cantilevers (Nanosensors) with a normal spring constant of about 30 N/m and a resonant frequency of about 260 kHz were used. The size of the cantilever tips (radius of curvature) is about 20 nm according to the manufacturer. The cantilever was excited just below its resonant frequency. All AFM measurements were performed in tapping mode at a scan rate of 0.5 Hz in air under ambient conditions. Transmission electron microscopic measurements of hybrid silica−lipid cylinders on carbon-coated grids were performed on a Tecnai F30 microscope with an accelerating voltage of 300 kV at room temperature. Reflection Fourier transform infrared (FT-IR) spectra of hybrid silica−lipid cylinders on Au-coated mica substrates were recorded with a Perkin-Elmer (100) spectrometer operating at 4 cm^{-1} resolution. Each spectrum represents an average of eight scans.

3. Results and Discussion

Figure 1a shows a height mode AFM image of a $DC_{8,9}PC$ tubule which was dried on a glass substrate. It can be seen that the tubule shows a cylindrical shape with a height of ∼450 nm (see the inset in Figure 1a), suggesting that the tubule is not compressed at the tip force employed for scanning and deformed by drying on the glass substrate. The apparent width of the tubule is broadened by the finite size of the AFM tip. The tubule surface appears to be uniform and smooth. There are no helical ripples observed in the height mode AFM image. Figure 1b is an amplitude mode AFM image of the tubule. This image was taken simultaneously with the height mode AFM image. Nanoscale helical ripples in the lipid tubule are clearly resolved in the amplitude mode. It is likely that the size and shape of the AFM tip limit the image resolution of the height mode. The better resolution in the amplitude mode is likely due to the edge enhancement. The sensitivity of the amplitude mode in imaging the nanoscale ripples of planar lipid bilayers has been also reported in the literature.[22] The pitch of the helical ripples in the lipid tubule measured from the amplitude mode image is ∼170 nm (see the inset in Figure 1b). The pitch angle of the helical ripples with respect to the equator of the lipid tubule is ∼28°. Because the helical ripples in the lipid tubule are not visible in the height mode image, their amplitudes are unknown.

It was found that the deposition and condensation of TEOS on $DC_{8,9}PC$ tubules in acidic solution at pH 2.0 for 1 week at room temperature lead to the sedimentation of $DC_{8,9}PC$ tubules to the bottom of glass tubes as a white solid. Figure 2a shows a dark field TEM image of a silica-coated lipid tubule dried on a carbon-coated grid. Nanoscale helical ripples are clearly observed. The chemical composite of the hybrid silica−lipid cylinder was analyzed by energy-dispersive X-ray microanalysis (EDX). The presence of Si and P in the hybrid silica−lipid cylinder is confirmed (Figure 2b). The pitch and pitch angle of the helical ripples in the templated silica cylinder are ∼170 nm and ∼43°, respectively. Our previous studies showed that the pitch of the helical ripples is 200 ± 30 nm for $DC_{8,9}PC$ tubules with diameters in the range from 200 to 650 nm, while the pitch angle of the helical ripples is in the range from 0 to 45°.[20] The results shown in Figure 2 suggest that the silica cylinders formed through the sol−gel reaction of TEOS replicate the lipid tubules with nanometer precision.

The hybrid silica−lipid cylinders retain their hollow cylindrical geometries after thermal treatment at 110 °C in air for 2 h. Figure 3a shows a TEM image of a thermally treated hybrid silica−lipid cylinder on a carbon-coated grid. The TEM image was taken at room temperature. As can be seen, both near and far sides of helical ripples are visible simultaneously, producing a network pattern in the TEM image. By examining the end of a thermally treated hybrid silica−lipid cylinder with TEM, we find that the hybrid silica−lipid cylinder is still hollow (Figure 3b). Although we are unable to resolve the silica distribution in the wall of the hybrid silica−lipid cylinder from the TEM image, it is likely that the silica film is formed on both inner and outer surfaces of the hollow lipid tubule because both inner and outer surfaces of the hybrid silica−lipid cylinder appear to be continuous and smooth. There are no residues from the thermally degraded lipid tubules observed inside the hollow cylinders. The control experiments showed that pristine $DC_{8,9}PC$ tubules lost their stability at ∼47 °C. When pristine $DC_{8,9}PC$ tubules were heated in air at 110 °C for 2 h, they were completely collapsed and broken into small pieces (Figure 4). It is clear that the deposition of the silica film improves the thermal stability of $DC_{8,9}PC$ tubules.

Figure 5 shows FT-IR spectra of thermally treated hybrid silica−lipid cylinders which were dried on an Au-coated mica substrate. The FT-IR spectra were taken at room temperature after thermal treatment at 110 °C in air for 2 h. In the region from 3000 to 2800 cm^{-1} (Figure 5a), we observe two bands at 2916 and 2849 cm^{-1}, respectively. They can be straightforwardly assigned to the asymmetric and symmetric stretching vibrations of the CH_2 in the acyl chains of $DC_{8,9}PC$ molecules. The stretch frequency and the full width at half-maximum of the CH_2 symmetric stretching are in good agreement with the earlier reports of infrared spectra for $DC_{8,9}PC$ tubules in solution at room temperature by Rudolph and Burke.[23] They found that the asymmetric and symmetric stretching vibrations of the CH_2 in $DC_{8,9}PC$ tubules started to shift at 47 °C. This suggests that the deposition of the silica films improves the thermal stability of lipid tubules and the lipid bilayer wall confining the hybrid silica−lipid cylinders retains its crystalline structure after the thermal process. The bands at 968, 804, and 719 cm^{-1} correspond to C−C stretching, C−H bending, and CH_2 rocking, respectively. It is known that Si−O−Si vibration band appears as a broad feature between 1000 and 1200 cm^{-1}. In the region between 700 to 1500 cm^{-1} (Figure 5b), we observe an intense band with a maximum at 1084 cm^{-1}, with a shoulder at 1200 cm^{-1}, which is consistent with the formation of highly cross-linked Si−O−Si networks on $DC_{8,9}PC$ tubules.

It is known that the $DC_{8,9}PC$ lipid is zwitterionic rather than charged, so the deposition of TEOS on $DC_{8,9}PC$ tubules cannot be explained by charge interactions. Mann and co-workers suggested that Br^- counterions served as a bridge for the deposition of positively charged TEOS on zwitterionic $DC_{8,9}$-

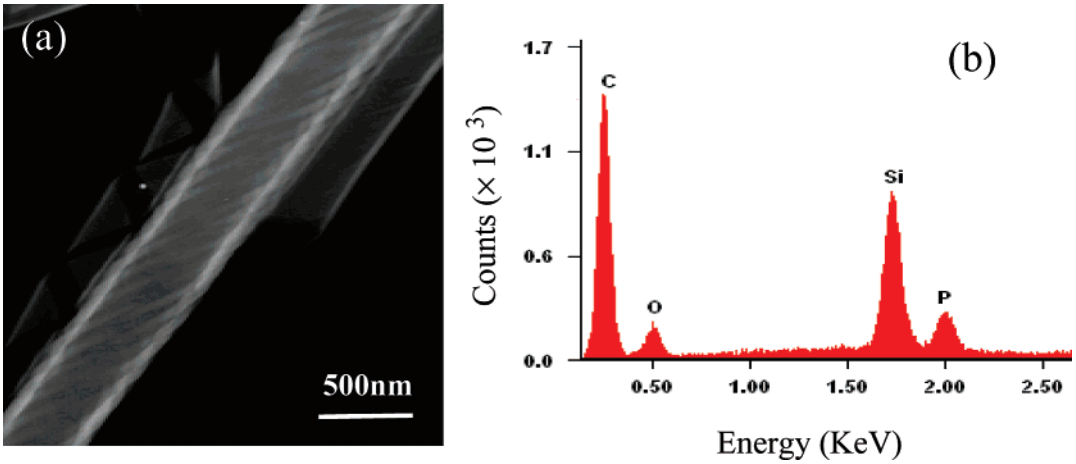

Figure 2. (a) Dark field TEM image of hybrid silica−lipid cylinders with nanoscale helical ripples. (b) EDX of hybrid silica−lipid cylinders. The hybrid silica−lipid cylinders were dried on carbon-coated grids. The TEM image was taken at room temperature.

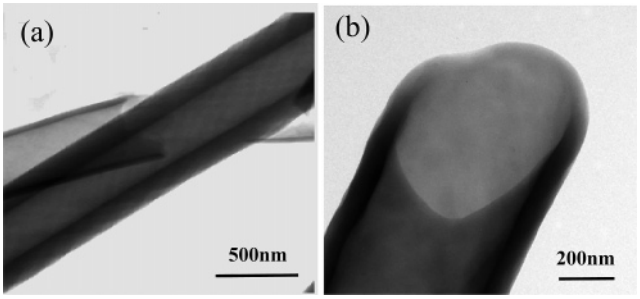

Figure 3. Bright field TEM images of hybrid silica−lipid cylinders with helical ripples (a) and an opened end (b). The hybrid silica−lipid cylinders were dried on carbon-coated grids and then were heated to 110 °C for 2 h. These TEM images were taken at room temperature.

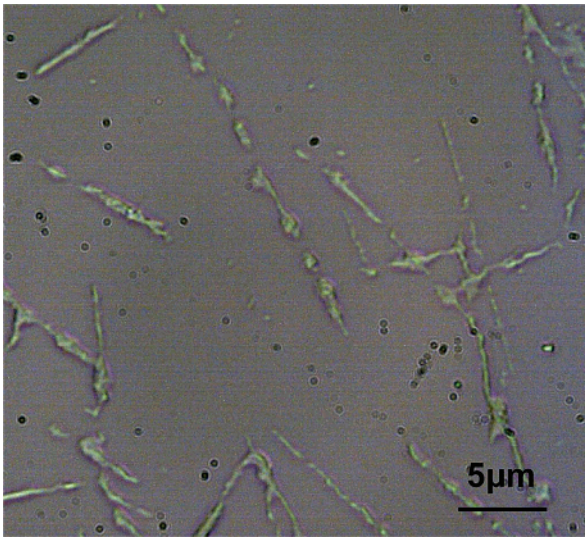

Figure 4. Optical microscopy image of lipid tubules which were dried on a glass substrate and then heated to 110 °C for 2 h.

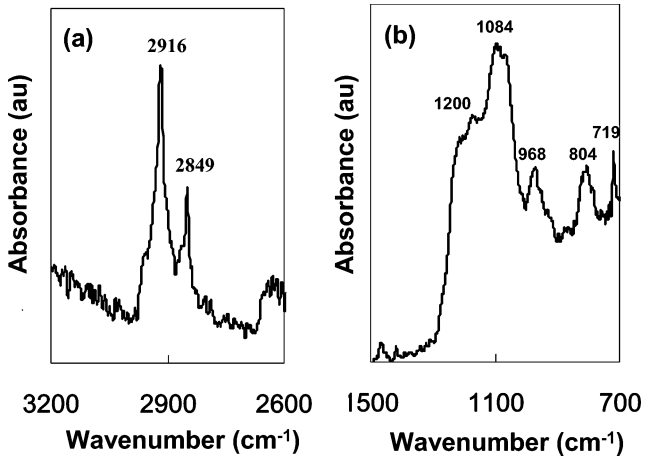

Figure 5. FT-IR spectra of hybrid silica−lipid tubules placed on Au-coated mica. (a) Region between 3200 and 2600 cm^{-1}. (b) Region between 1500 and 70 cm^{-1}. The hybrid silica−lipid cylinders were dried on Au-coated mica and then were heated to 110 °C for 2 h. The spectra represent an average of four scans taken with a 2 cm^{-1} resolution at room temperature.

PC lipids in HBr aqueous solution.[16] In our experiments, The deposition and condensation of TEOS on $DC_{8,9}PC$ tubules were carried out in HCl aqueous solution. However, the presence of Cl^- counterions in the hybrid lipid−silica cylinders is not confirmed by EDX (Figure 2b). On the other hand, the curvature of bilayer membranes is known to induce a net electrostatic polarization normal to the membrane, producing a flexoelectric effect.[24] The curvature of a cylindrical lipid tubule can lead a polarization of $\sim 10^{-12}$ C/m.[25] The flexoelectric effect of lipid tubules should have a substantial impact on the adsorption of charged particles on their surfaces. It is known that under acid condition the alkoxide groups of TEOS are protonated.[26] We speculate that the deposition of positively charged TEOS on the $DC_{8,9}PC$ tubules in HCl aqueous solution at pH 2.0 is due to the flexoelectric effect. The condensation of the deposited TEOS leads to the formation of silica films on helical rippled $DC_{8,9}PC$ tubules.

In conclusion, we report the sol−gel condensation of tetraethoxysilane (TEOS) on helical rippled lipid tubules of 1,2-bis(tricosa-10,12-diynoyl)-*sn*-glycero-3-phosphocholine ($DC_{8,9}$PC). Transmission electron microscopy reveals that the nanoscale helical ripples of the lipid tubules are transcripted to the templated silica films. The deposition of the silica film substantially improves the thermal stability of lipid tubules. We find that the crystalline ordering of lipid bilayer walls confined in the hybrid silica−lipid cylinders is stable up to 110 °C. Compared with the smooth silica cylinders, the helical rippled silica cylinders have a large surface area. The hybrid silica−lipid cylinders with nanoscale helical rippling might have potential applications in heterogeneous chiral catalysis and separation.

Acknowledgment. We acknowledge Drs. Jianhua Zou and Qun Huo for help in the FT-IR measurements.

References and Notes

(1) Whitesides, G. M.; Mathias, J. P.; Seto, C. T. *Science* **1991**, *254*, 1312.
(2) Ying, J. Y.; Mehnert, C. P.; Wong, M. S. *Angew. Chem., Int. Ed.* **1999**, *38*, 56.
(3) van Bommel, K. J. C.; Friggeri, A.; Shinkai, S. *Angew. Chem., Int. Ed.* **2003**, *42*, 980.
(4) Schnur, J. M. *Science* **1993**, *262*, 1669.
(5) Shimizu, T.; Masuda, M.; Minamikawa, H. *Chem. Rev.* **2005**, *105*, 1401.
(6) Archibald, D. D.; Mann, S. *Nature* **1993**, *364*, 430.
(7) Jung, J. H.; Kobayashi, H.; Masuda, M.; Shimizu, T.; Shinkai, S. *J. Am. Chem. Soc.* **2001**, *123*, 8785.
(8) Price, R. R.; Dressick, W. J.; Singh, A. *J. Am. Chem. Soc.* **2003**, *125*, 11259.
(9) Patil, A. J.; Muthusamy, E.; Seddon, A. M.; Mann, S. *Adv. Mater.* **2003**, *15*, 1816.
(10) Dang, T. X.; Farah, S. J.; Gast, A.; Robertson, C.; Carragher, B.; Egelman, E.; Wilson-Kubalek, E. M. *J. Struct. Biol.* **2005**, *150*, 90.
(11) Zhou, Y.; Ji, Q.; Masuda, M.; Kamiya, S.; Shimizu, T. *Chem. Mater.* **2006**, *18*, 403.
(12) Zhao, Y.; Mahaja, N.; Fang, J. F. *Small* **2006**, *2*, 364.
(13) Baral, S.; Schoen, P. *Chem. Mater.* **1993**, *5*, 145.
(14) Jung, J. H.; Lee, S. H.; Yoo, J. S.; Yoshida, K.; Shimizu, T.; Shinkai, S. *Chem.—Eur. J.* **2003**, *9*, 5307.
(15) Ji, Q.; Iwaura, R.; Kogiso, M.; Jung, J. H.; Yoshida, K.; Shimizu, T. *Chem. Mater.* **2004**, *16*, 250.
(16) Seddon, A. M.; Patel, H. M.; Burkett, S. L.; Mann, S. *Angew. Chem., Int. Ed.* **2002**, *41*, 2988.
(17) Nagle, J. F.; Tristram-Nagel, S. *Biochim. Biophys. Acta* **2000**, *1469*, 159.
(18) Selinger, J. V.; Spector, M. S.; Schnur, J. M. *J. Phys. Chem. B* **2001**, *105*, 7157.
(19) Zhao, Y.; Mahajan, N.; Lu, R.; Fang, J. Y. *Proc. Natl, Acad. Sci. U.S.A.* **2005**, *102*, 7438.
(20) Mahajan, N.; Zhao, Y.; Du, T.; Fang, J. Y. *Langmuir* **2006**, *22*, 1973.
(21) Lauf, U.; Fahr, A.; Westesen, K.; Ulrich, A. S. *ChemPhysChem* **2004**, *5*, 1246.
(22) Leidy, C.; Kaasgaard, T.; Crowe, J. H.; Mouritsen, O. G.; Jøegensen, K. *Biophys. J.* **2002**, *83*, 2625.
(23) Rudolph, A. S.; Burke, T. G. *Biochim. Biophys. Acta* **1987**, *902*, 349.
(24) Petrov, A. G.; Spassova, M.; Fendler, J. H. *Thin Solid Films* **1996**, *285*, 845.
(25) Lvov, Y. M.; Price, R. R.; Selinger, J. V.; Singh, A.; Spector, M. S.; Schnur, J. M. *Langmuir* **2000**, *16*, 5932.
(26) Brinker, C. J.; Schere, G. W. *Sol-Gel Science. The Physics and Chemistry of Sol-Gel Processing*; Academic Press: New York, 1990.